Distribution of high-stability 100.04 GHz millimeter wave signal over 60 km optical fiber with fast phase-error-correcting capability

Dongning Sun, Yi Dong,* Hongxiao Shi, Zongyang Xia, Zhangweiyi Liu, Siwei Wang, Weilin Xie, and Weisheng Hu

State Key Laboratory of Advanced Optical Communication Systems and Networks, Shanghai Jiao Tong University, 800 Dong Chuan Road, Shanghai 200240, China
*Corresponding author: yidong@sjtu.edu.cn

We demonstrate a phase-stabilized remote distribution of 100.04 GHz millimeter wave signal over 60 km optical fiber. The phase error of the remote millimeter wave signal induced by fiber transmission delay variations is detected by dual-heterodyne phase error transfer and corrected with a feedback system based on a fast response acousto-optic frequency shifter. The phase noise within the bandwidth of 300 Hz is effectively suppressed; thus, the fast transmission delay variations can be compensated. The residual phase noise of the remote 100.04 GHz signal reaches −56 dBc/Hz at 1 Hz frequency offset from the carrier, and long-term stability of 1.6×10^{-16} at 1000 s averaging time is achieved. The fast phase-noise-correcting capability is evaluated by vibrating part of the transmission fiber link.   © 2014 Optical Society of America

OCIS codes: (060.2330) Fiber optics communications; (060.5625) Radio frequency photonics; (070.1170) Analog optical signal processing.
http://dx.doi.org/10.1364/OL.39.002849

Remote distribution of local stable signals over optical fiber has attracted growing research interest in recent years due to its extensive applications, including very long baseline interferometers [1,2], particle accelerators [3], and remote clock synchronization and comparison [4,5]. In deep space networks and phase-array millimeter-wave (mm-wave) antennas, distribution of mm-wave reference with high phase stability is indispensable [6–8]. For example, with the Atacama Large Millimeter Array (ALMA), its highest receiving frequency reaches 950 GHz [9]. In order to receive such high frequencies, a high reference frequency is required for the remote site, and the reference signal of different antennas has to be highly stable for maintaining signal coherency [10,11].

However, the transmission delay varies due to environmental perturbations on fiber links, which degrade phase stability at the remote end. A fiber stretcher is widely applied to correct the transmission delay in the fiber [12–14]. Although its frequency independent compensation enables distribution of high frequency references directly, its small compensation range and slow response limit the system's loop bandwidth and application in transmission systems that suffer large and fast variation of the transmission delay. Recently, a work reported transferring an 80 GHz signal over a 10 km fiber with phase correction using a fiber stretcher [11,13]. Voltage-controlled oscillators (VCOs), an alternative phase error correcting method, have an infinite compensation range and fast response, and several VCO-based distribution systems have been reported [15,16]. However, it is difficult to distribute even tens of GHz local reference due to the band-limited frequency range of phase detection and limited phase control accuracy of high frequency VCO. Thus, as far as we know, some research on VCO-based systems mainly focuses on transmission of several GHz or approximately 10 GHz signals [17–19].

In this Letter, we demonstrate a phase-stabilized remote distribution of a 100.04 GHz millimeter wave signal over 60 km optical fiber based on the ideas in [20]. These ideas consist of high-frequency phase detection and precise phase control by dual-heterodyning phase error transfer (DHPT) and an acousto-optic frequency shifter (AOFS), respectively. The transmitted mm-wave signal over the fiber link is obtained by extracting two optical carriers from an optical frequency comb (OFC). With active compensation, the residual phase noise of a remote mm-wave signal is −26 dBc/Hz and −56 dBc/Hz at 0.01 Hz and 1 Hz frequency offset from the carrier, respectively, and the long term stability of 1.6×10^{-16} at 1000 s averaging time is achieved. Thanks to the fast response of AOFS-based phase corrections, the system's loop bandwidth reaches about 300 Hz. Thus, the fast transmission delay variations can be corrected, which is evaluated by vibrating part of the transmission fiber link.

The experimental setup of the mm-wave signal distribution system is shown in Fig. 1. The local end and the remote end are connected by a 60 km spooled single-mode optic fiber cable. A 500 m long optical fiber vibrating at 6 Hz by using a mechanical vibrator is inserted in the transmission link to evaluate the capability of correcting fast transmission delay variations. A dispersion compensating fiber (DCF) module is added to the end of the optical fiber to compensate its dispersion. An optical frequency comb generator (OFCG) based on a Fabry–Perot electro-optic modulator with 2.5 GHz free spectral range (FSR) is driven by a 25 GHz microwave synthesizer, which produces a low phase noise OFC with a 25 GHz frequency interval and more than a 10 THz spectral span. The OFC is divided into four branches (A, B, C, and D) by passing through polarization maintaining couplers PMC1 to PMC3. The A branch is used to obtain two phase-locked optical carriers with 100.04 GHz frequency

spacing as described in [20]. The B branch is used to measure the residual phase noise of the remote end mm wave signal. The C branch is reference for detecting phase error induced by two separated paths "a" and "b" of polarization maintaining arrayed waveguide grating (PM-AWG) with 25 GHz spacing used to select two spectral lines of the OFC, and the D branch is reference for detecting the 60 km transmission link induced phase error. The generated mm-wave signals are power split into two branches by PMC4. One branch is combined with reference C and the other one is transmitted to the remote end. The remote optical signals are power split into three branches by optical couplers OC1 and OC2. One is used to obtain 100.04 GHz mm-wave signal by a high-speed photo-detector (PD). Another one is used to measure phase noise at the remote end. The third one is frequency up-shifted 35 MHz by AOFS3 and transmitted back to the local end through the same fiber link. This frequency up-shift can distinguish the roundtrip signal from back-scattered signals. To compensate the optical loss caused by transmission links, two erbium-doped optical fiber amplifiers (EDFAs) are employed before and after transmission. At both ends of the optical transmission link, optical circulators (C1, C2) are used to distinguish the transmitted and received signals.

Since the 60 km fiber link is suffering a time-varying transmission delay $\tau_{\text{trans}}(t)$, the mm-wave signal obtained at the remote end can be written as

$$I_{\text{mm}}(t) = \cos[(\omega_2 - \omega_1 + \omega_{\text{IF2}})t + \varphi_v(t) + \varphi_p(t)], \quad (1)$$

where

$$\varphi_p(t) = -[(\omega_2 + \omega_{\text{IF1}} + \omega_{\text{IF2}})\tau_b(t) - (\omega_1 + \omega_{\text{IF1}})\tau_a(t)]$$
$$- (\omega_2 - \omega_1 + \omega_{\text{IF2}})\tau_{\text{trans}}(t).$$

$\varphi_p(t)$ is phase fluctuation induced by time varying delays of the two separated paths and the 60 km fiber link, ω_1 and ω_2 are the two extracted comb lines' angular frequency, ω_{IF1} and ω_{IF2} are angular frequency of the intermediate frequency signals IF1 and IF2, $\varphi_v(t)$ is instantaneous phase of the IF2 signal, and $\tau_a(t)$ and $\tau_b(t)$ are time varying transmission delays of the separated path "a" and "b." Therefore, in order to receive a phase stable mm-wave signal at the remote end, the $\varphi_v(t)$ is driven by a feedback network to compensate the optical fiber links' induced phase fluctuations.

The active phase compensation is realized as follows: At the local end, a 40 MHz beating signal is obtained in DHPT1, whose phase represents the phase fluctuations caused by the separated path "a" and "b." It can be expressed as

$$V_{\Delta ab}(t) = \cos\{\omega_{\text{IF2}}t + \varphi_v(t)$$
$$- [(\omega_2 + \omega_{\text{IF1}} + \omega_{\text{IF2}})\tau_b(t) - (\omega_1 + \omega_{\text{IF1}})\tau_a(t)]\}.$$
$$(2)$$

The returned optical carriers shown as green lines in the insets of Fig. 1 exhibit a double transmission delay. They are heterodyned with original OFC (reference D), generating beating signals of 70 and 110 MHz that are mixed to generate a 40 MHz signal in DHPT2. It is expressed as
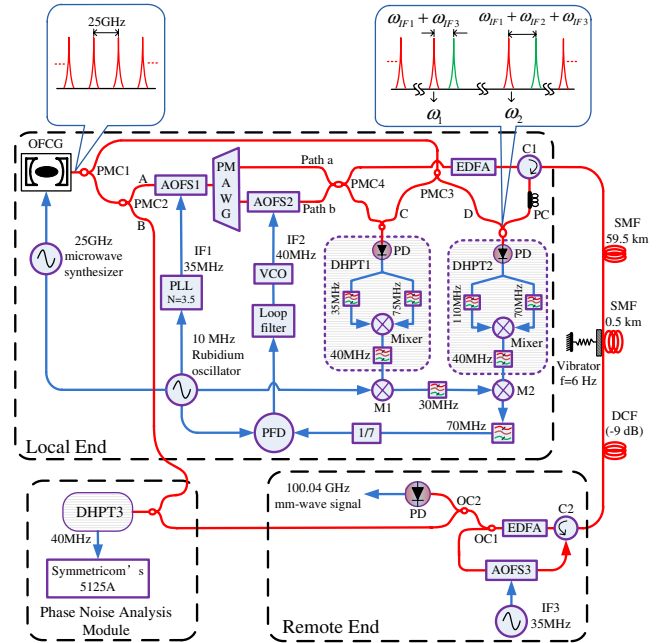

Fig. 1. Experimental setup for stable dissemination millimeter-wave signal system. OFCG, optical frequency comb generator; PMC, polarization-maintaining coupler; PLL, phase-locked loop; OC, optical coupler; AOFS, acousto-optic frequency shifter; IF, intermediate frequency; PM-AWG, polarization maintaining arrayed waveguide grating; VCO, voltage controlled oscillator; EDFA, erbium-doped optical fiber amplifier; DHPT, dual-heterodyne phase error transfer; PD, photodetector; PFD, digital phase and frequency detector; PC, polarization controller; SMF, single-mode fiber; DCF, dispersion compensating fiber; M, mixer; C, circulator.

$$V_{\Delta\text{trans}}(t)$$
$$= \cos\{\omega_{\text{IF2}}t - (\omega_2 + \omega_{\text{IF1}} + \omega_{\text{IF2}})[\tau_b(t) + 2\tau_{\text{trans}}(t)]$$
$$+ (\omega_1 + \omega_{\text{IF1}})[\tau_a(t) + 2\tau_{\text{trans}}(t)] + \varphi_v(t)\}. \quad (3)$$

In order to avoid interference of harmonics during the mixing, $V_{\Delta ab}(t)$ is mixed with the 10 MHz rubidium oscillator in mixer1 (M1) to obtain a 30 MHz down-converted signal that then multiplies the $V_{\Delta\text{trans}}(t)$ in mixer2 (M2). Thus, a 70 MHz up-converted signal can be obtained and written as

$$V_{70\,\text{MHz}}(t) = \cos[(2\omega_{\text{IF2}} - \omega_{Rb})t + 2\varphi_v(t) - \varphi_{Rb}$$
$$-2(\omega_2 + \omega_{\text{IF1}} + \omega_{\text{IF2}})[\tau_b(t) + \tau_{\text{trans}}(t)]$$
$$+2(\omega_1 + \omega_{\text{IF1}})[\tau_a(t) + \tau_{\text{trans}}(t)], \quad (4)$$

where ω_{Rb} is the angular frequency of 10 MHz rubidium oscillator and φ_{Rb} is its initial phase and considered as a constant. After sevenfold dividing of $V_{70\,\text{MHz}}(t)$ and comparing with the rubidium oscillator, the phase error signal discriminated by a digital phase and frequency detector (PFD) can be obtained:

$$E_{\text{error}}(t) = \varphi_{Rb} - \frac{1}{7}\{2\varphi_v(t) - \varphi_{Rb}$$
$$+ 2(\omega_1 + \omega_{\text{IF1}})[\tau_a(t) + \tau_{\text{trans}}(t)]$$
$$-2(\omega_2 + \omega_{\text{IF1}} + \omega_{\text{IF2}})[\tau_b(t) + \tau_{\text{trans}}(t)]\}. \quad (5)$$

The error signal is integrated in a loop filter to control the phase of VCO. When the phase-locked loop is locked, the steady state error is zero, i.e., $E_{\text{error}}(t) \to 0$. Then, the obtained mm-wave signal at the remote end can be expressed as

$$I_{\text{mm}}(t) = \cos[(\omega_2 - \omega_1 + \omega_{\text{IF2}})t + 4\varphi_{Rb}]. \quad (6)$$

From Eq. (6), it can be seen that $I_{\text{mm}}(t)$ is independent of the time-varying transmission delay induced by the separated paths and the transmission link. Thus, a phase stable 100.04 GHz mm-wave signal is obtained at the remote end.

As shown in the phase noise analysis module of Fig. 1, reference B is optical heterodyned with the remote optical carriers, thus obtaining a 40 MHz beating signal from DHPT3. According to the DHPT scheme [20], the phase noise performance of remote mm-wave signal can be evaluated by measuring this 40 MHz signal with a phase noise analyzer (Symmetricom's 5125A). Figure 2 shows measured results of the 60 km transmission system in conditions of the free running (without phase compensation, VCO directly locked to rubidium oscillator), the phase locking (loop bandwidth about 300 Hz), and phase locked 1 m optical fiber transmission link. Comparing the phase noise of the free-running and phase-locked 60 km transmission system, it can be seen that the phase noise induced by transmission links is mainly within the 10 Hz frequency. In the phase-locked 60 km transmission system, the phase noise is reduced from 32 to −26 dBc/Hz and −35 to −56 dBc/Hz at 0.01 and 1 Hz frequency offset from the carrier, respectively, approaching that of a 1 m optical fiber system. The phase noise of 60 km system exceeds that of 1 m optical fiber systems at above 3 Hz, mainly due to correlated phase noise of the microwave signal and its long distance-delayed signal. Additionally, the spur at 600 Hz comes from the microwave synthesizer. The superimposed waveforms of remote 40 MHz beating signals in free running and phase-locked systems are measured in 10 s and 30 min, respectively, by using a digital storage oscilloscope trigger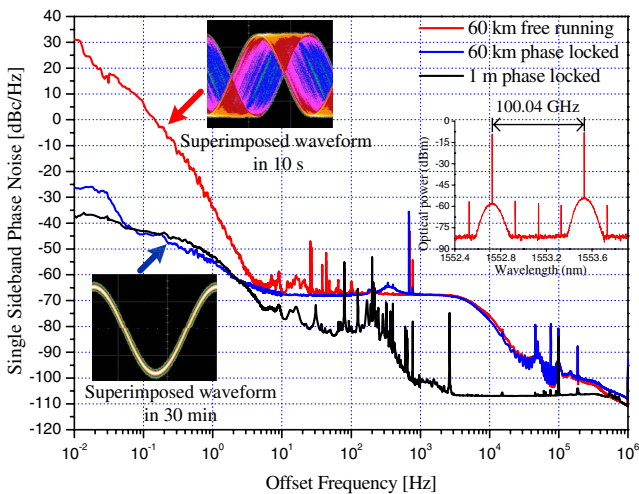ed by the rubidium oscillator. As shown in insets of Fig. 2, the waveform of the free running system is totally in mess even in 10 s, which severely deteriorates the phase performance of the remote mm-wave signal. The optical spectrum of the 100.04 GHz signal before detection is also shown in the insets of Fig. 2.

Figure 3 shows the results of the inserted 500 m fiber vibrating at 6 Hz under different vibrational amplitude (Va). As Va increases from 4 to 10 mm, a bunch of spurs arise at high-order harmonics frequency of 6 Hz. Therefore, a wide loop bandwidth is desired for practical long distance transmission. It can be seen that the phase-locked 60 km transmission system effectively suppresses the phase noise within the loop bandwidth (approximately 300 Hz), as shown in the blue line, which exhibits the fast phase-error-correction capability.

The frequency stability of the remote signal is shown in Fig. 4. The 60 km transmission system's stability in free running system is 1.8×10^{-13} at 1000 s averaging time. The phase-locked system reduces frequency instability by three orders of magnitude to 1.6×10^{-16} at 1000 s averaging time. It can be seen that the frequency stability of phase-locked system is approaching a 1 m optical fiber transmission system. Vibration has no significant effect on the frequency stability of phase locked system. This demonstrates the effectiveness of our compensation system and ensures the stability of remote signal in long term transmission.

In conclusion, a highly phase stable mm-wave signal distribution system with fast phase-error-correcting capability was experimentally demonstrated in this Letter. A 100.04 GHz signal over optical fiber is extracted from an OFC and stably transmitted over 60 km fiber links. The phase error induced by fiber transmission delay variations is detected by DHPT and corrected with a fast response AOFS-based feedback system. The residual phase noise of the phase-locked 60 km transmission system is −26 dBc/Hz and −56 dBc/Hz at 0.01 and 1 Hz frequency offset from the carrier, respectively. Frequency stability achieves 1.6×10^{-16} at 1000 s averaging time. Additionally, the inserted 500 m fiber vibrating at 6 Hz under different vibrational amplitude experimentally demonstrates the fast phase error correcting capability

Fig. 2. Residual phase noise of remote 100.04 GHz signal is evaluated without vibration.
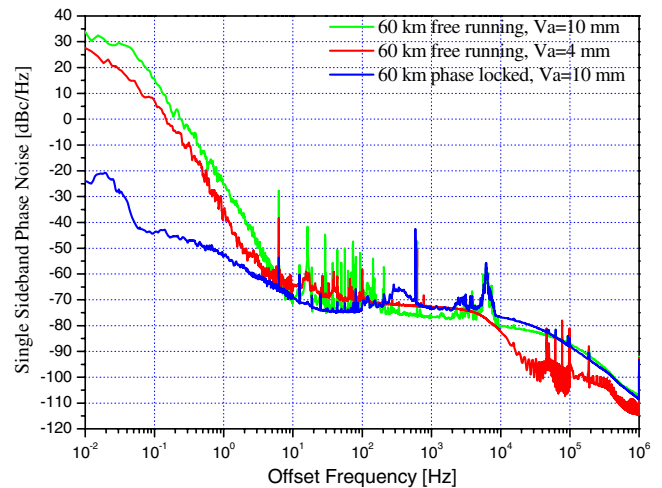

Fig. 3. Residual phase noise of remote 100.04 GHz signal is evaluated with vibration (vibrational frequency 6 Hz).
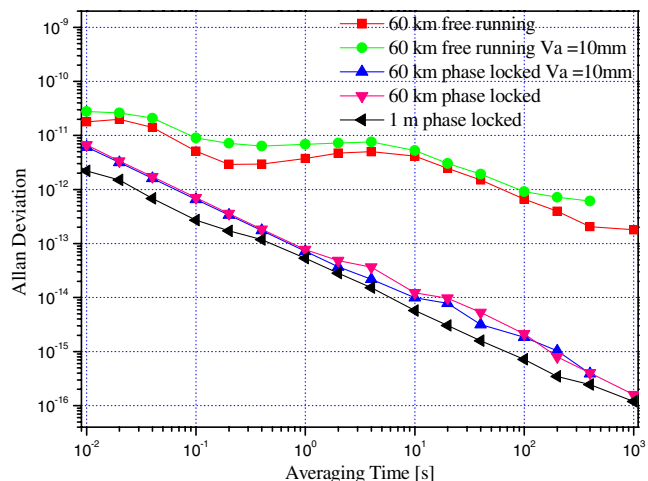
Fig. 4.   Allan deviation with vibration and without vibration.

of the system, which is essential to stable distribution of high frequency reference in long distance transmission link.

References

1. K. Sato, T. Hara, S. Kuji, K. Asari, M. Nishio, and N. Kawano, IEEE Trans. Instrum. Meas. **49**, 19 (2000).
2. M. Tarenghi, Astrophys. Space Sci. **313**, 1 (2008).
3. P. R. Bolton, Int. J. Mod. Phys. B **21**, 527 (2007).
4. Y. F. Chen, J. Jiang, and D. J. Jones, Opt. Express **14**, 12134 (2006).
5. J. Ye, J. L. Peng, R. J. Jones, K. W. Holman, J. L. Hall, D. J. Jones, S. A. Diddams, J. Kitching, S. Bize, J. C. Bergquist, L. W. Hollberg, L. Robertsson, and L. S. Ma, J. Opt. Soc. Am. B **20**, 1459 (2003).
6. M. Calhoun, S. Huang, and R. L. Tjoelker, Proc. IEEE **95**, 1931 (2007).
7. J. M. Payne, L. D'Addario, D. T. Emerson, A. R. Kerr, and B. Schillue, Proc. SPIE **3357**, 143 (1998).
8. G. L. Pilbratt, J. R. Riedinger, T. Passvogel, G. Crone, D. Doyle, U. Gageur, A. M. Heras, C. Jewell, L. Metcalfe, S. Ott, and M. Schmidt, Astron. Astrophys. **518**, L1 (2010).
9. J. Cliche and B. Shillue, IEEE Control Syst. Mag. **26**(1), 19 (2006).
10. B. Shillue, S. AlBanna, and L. D'Addrio, in *Proceedings of IEEE International Topical Meeting on Microwave Photonics (MWP)* (IEEE, 2004), pp. 201–204.
11. H. Kiuchi and T. Kawanishi, in *Proceedings of IEEE Conference on General Assembly and Scientific Symposium* (IEEE, 2011), pp. 1–4.
12. G. Marra, R. Slavík, H. S. Margolis, S. N. Lea, P. Petropoulos, D. J. Richardson, and P. Gill, Opt. Lett. **36**, 511 (2011).
13. H. Kiuchi, IEEE Trans. Microwave Theory Tech. **56**, 1493 (2008).
14. O. Lopez, A. Amy-Klein, M. Lours, and C. Chardonnet, Appl. Phys. B **98**, 723 (2010).
15. M. Kumagai, M. Fujieda, S. Nagano, and M. Hosokawa, Opt. Lett. **34**, 2949 (2009).
16. M. Fujieda, M. Kumagai, T. Gotoh, and M. Hosokawa, IEEE Trans. Instrum. Meas. **58**, 1223 (2009).
17. M. Fujieda, M. Kumagai, and S. Nagano, IEEE Trans. Ultrason. Ferroelectr. Freq. Control **57**, 168 (2010).
18. B. Wang, C. Gao, W. L. Chen, J. Miao, X. Zhu, Y. Bai, J. W. Zhang, Y. Y. Feng, T. C. Li, and L. J. Wang, Sci. Rep. **2**, 556 (2012).
19. S. Wang, D. Sun, Y. Dong, W. Xie, H. Shi, L. Yi, and W. Hu, Opt. Lett. **39**, 888 (2014).
20. D. Sun, Y. Dong, L. Yi, S. Wang, H. Shi, Z. Xia, W. Xie, and W. Hu, Opt. Lett. **39**, 1493 (2014).